UDC 621.3 **doi: 10.20998/2074-272X.2020.6.07**

R. Kouadri, L. Slimani, T. Bouktir

SLIME MOULD ALGORITHM FOR PRACTICAL OPTIMAL POWER FLOW SOLUTIONS INCORPORATING STOCHASTIC WIND POWER AND STATIC VAR COMPENSATOR DEVICE

Purpose. This paper proposes the application procedure of a new metaheuristic technique in a practical electrical power system to solve optimal power flow problems, this technique namely the slime mould algorithm (SMA) which is inspired by the swarming behavior and morphology of slime mould in nature. This study aims to test and verify the effectiveness of the proposed algorithm to get good solutions for optimal power flow problems by incorporating stochastic wind power generation and static VAR compensators devices. In this context, different cases are considered in order to minimize the total generation cost, reduction of active power losses as well as improving voltage profile. Methodology. The objective function of our problem is considered to be the minimum the total costs of conventional power generation and stochastic wind power generation with satisfying the power system constraints. The stochastic wind power function considers the penalty cost due to the underestimation and the reserve cost due to the overestimation of available wind power. In this work, the function of Weibull probability density is used to model and characterize the distributions of wind speed. Practical value. The proposed algorithm was examined on the IEEE-30 bus system and a large Algerian electrical test system with 114 buses. In the cases with the objective is to minimize the conventional power generation, the achieved results in both of the testing power systems showed that the slime mould algorithm performs better than other existing optimization techniques. Additionally, the achieved results with incorporating the wind power and static VAR compensator devices illustrate the effectiveness and performances of the proposed algorithm compared to the ant lion optimizer algorithm in terms of convergence to the global optimal solution. References 38, tables 6, figures 9.
Key words: **optimal power flow, slime mould algorithm, stochastic wind power generation, static VAR compensators.**

Мета. У статті пропонується процедура застосування нового метаевристіческого методу в реальній електроенергетичній системі для розв'язання задач оптимального потоку енергії, а саме алгоритму слизової цвілі, який заснований на поведінці рою і морфології слизової цвілі в природі. Дане дослідження спрямоване на тестування і перевірку ефективності запропонованого алгоритму для отримання хороших рішень для проблем оптимального потоку потужності шляхом включення пристроїв стохастичною вітрової генерації і статичних компенсаторів VAR. У зв'язку з цим, розглядаються різні випадки, щоб мінімізувати загальну вартість генерації, знизити втрати активної потужності і поліпшити профіль напруги. Методологія. В якості цільової функції завдання розглядається мінімальна сукупна вартість традиційної генерації електроенергії і стохастичної вітрової генерації при задоволенні обмежень енергосистеми. Стохастична функція енергії вітру враховує величини штрафів через недооцінку і резервні витрати через завищену оцінку доступної вітрової енергії. У даній роботі функція щільності ймовірності Вейбулла використовується для моделювання і характеристики розподілів швидкості вітру. Практична цінність. Запропонований алгоритм був перевірений на системі шин IEEE-30 і великий алжирської тестовій енергосистемі зі 114 шинами. У випадках, коли мета полягає в тому, щоб звести до мінімуму традиційне вироблення електроенергії, досягнуті результати в обох тестових енергосистемах показали, що алгоритм слизової цвілі функціонує краще, ніж інші існуючі методи оптимізації. Крім того, досягнуті результати з використанням вітрової енергії і статичного компенсатора VAR ілюструють ефективність і продуктивність запропонованого алгоритму в порівнянні з алгоритмом оптимізатора мурашиних левів з точки зору збіжності до глобального оптимального рішення. Бібл. 38, табл. 6, рис. 9.
Ключові слова: **оптимальний потік енергії, алгоритм слизової цвілі, стохастична генерація енергії вітру, статичні VAR компенсатори.**

Introduction. In the last decade, energy consumption has been increased significantly especially in developing countries. Renewable energy can be known as green energy or clean energy is one of the best solutions to the increasing demand problem, and it is inexhaustible energy that comes from natural resources or processes that are constantly replenished [1], even if their availability depends on weather and weather conditions, and whose exploitation causes the least possible ecological damage, does not cause toxic waste and does not cause damage to the environment. They are cleaner, more environmentally friendly than fossil fuels and fissile energies, environmentally friendly, available in large quantities around the world.

Nowadays, the integration of renewable energy sources – RESs (i.e., solar, wind, hydropower, etc.) into the electrical grid is experiencing a rapid increase. Among the various RESs, wind energy considered is one of the most desirable sources in recent years that keeps developing thanks to the technological advances made in the field of wind generators to reduce the cost of system installations. In addition, the application of flexible AC transmission systems (FACTS) controllers such as static VAR compensators (SVC) devices that considered one of the most controllers used in the case of the high demand for energy to maintain the magnitude of bus voltage at the desired level, improve voltage security and minimize the total power losses.

With the growing penetration of RESs in the power system, the study of optimal power flow (OPF) becomes necessary to solve power system problems or improve the performance of this system. The OPF for the system that includes RESs such as wind power generators is the subject of ongoing research models nowadays. It is necessary to confront the stochastic nature of this source for analysis of the planning and operation of modern power systems, in order to obtain much more precise

results [2]. In general, the problem with wind power is the stochastic nature of wind speed. Therefore the model which considers the probability of the available wind power can represent the cost of overestimating and underestimating this power at a certain period.

Recently, OPF with stochastic wind power has extensively been studied by more researchers. In [3] authors proposed a Gbest-guided artificial bee colony algorithm (GABC) to solve the OPF problem in the IEEE 30 bus system incorporating stochastic wind power. In attempting the same problem in [4] author proposed a modified moth swarm algorithm (MMSA) to solve the OPF problem incorporating stochastic wind power. In this work, three different objective functions are considered, which are the minimize the total operating cost, reduce the transmission power loss, and improve the voltage profile enhancement. In another study [5] authors applied the success history-based adaptation technique of differential evolution algorithm to solve the OPF problem comprises of stochastic wind-solar power with conventional thermal generators under various cases. The OPF incorporation with wind power and static synchronous compensator STATCOM was studied in [6] by using a modified bacteria foraging algorithm (MBFA). The results obtained proved that MBFA efficiency and better than the ACO algorithm for solving OPF problems in power systems. Bird Swarm Algorithm (BSA) for solving an OPF problem with incorporating stochastic wind and solar PV power in the power system is studied in [7]. The proposed approach applied in the modified IEEE 30-bus system with objective function is to minimize the total energy generation cost, which is the cost of thermal-wind-solar. In [8] authors applied a modified hybrid PSOGSA with a chaotic maps approach to improve OPF results by incorporating stochastic wind power and two controllers in the FACTS family such as TCSCs and TCPSs. The proposed method is applied in the power systems to minimize the thermal generators' fuel cost and the wind power generating cost.

Several metaheuristic optimization algorithms were developed and applied for the OPF solution. Some of them are: salp swarm optimizer [9], moth swarm algorithm [10], differential evolution [11], glowworm swarm optimization [12], differential search algorithm [12], moth-flame optimizer [14], stud krill herd algorithm [15], artificial bee colony algorithm [16], symbiotic organisms search algorithm [17], improved colliding bodies optimization algorithm [18], firefly algorithm [19], black-hole-based optimization approach [20], the league championship algorithm [21, 22], multi-verse optimizer [23], harmony search algorithm [24], earthworm optimization algorithm [25]. Among several numbers of the available metaheuristic algorithm, a new flexible and efficient stochastic optimization algorithm has been proposed to solve our problem and satisfy our imposed conditions, this technique namely a slime mould algorithm (SMA). SMA is based upon the oscillation mode in nature and simulates the swarming behavior and morphology of slime mould in foraging.

In this paper, a new flexible and efficient stochastic optimization algorithm called slime mould algorithm (SMA) has been proposed with the aim is solving the OPF problem in power systems incorporating stochastic wind power and SVC devices.

Modeling of SVC. The static VAR compensator (SVC) device is an important member of the FACTS controllers' family. The importance of SVC is to maintain the bus voltage magnitude at the desired level by providing or absorbing reactive energy. In the power system, SVC is modeled by shunt variable admittance. SVC's admittance only has its imaginary part since the SVC device's power loss is assumed to be negligible and is given as follows:

$$y_{SVC} = jb_{SVC}. \quad (1)$$

The b_{SVC} susceptance can be capacitive or inductive to provide or absorb reactive power, respectively. In this study, SVC is installed in the power system as a PV bus with the objective is to regulate the voltage magnitude V_k by injecting reactive power to a bus where it is connected. The current I_{SVC} and reactive power Q_{SVC} absorbed or injected by the SVC device is calculated as follow:

$$I_{SVC} = jb_{SVC}V_k; \quad (2)$$

$$Q_{SVC} = -V_k^2 b_{SVC}. \quad (3)$$

Optimal power flow problem formulation. The optimal power flow problem solution aims to give the optimum value of the objective function by adjusting the settings of control variables. Generally, the mathematical expression of the optimization problem with satisfying various equality and inequality constraints may be represented as follows:

$$\min F(\boldsymbol{x},\boldsymbol{u}); \quad (4)$$

$$\text{Subjected to } g(\boldsymbol{x},\boldsymbol{u}) = 0; \quad (5)$$

$$h(\boldsymbol{x},\boldsymbol{u}) \le 0; \quad (6)$$

where $F(x, u)$ denotes the objective function that to be optimized, $\boldsymbol{x}$ and $\boldsymbol{u}$ represents the vectors of the state variables (dependent variables) and control variables (independent variables), respectively.

Control variables. In the OPF the control variables should be adjusted to satisfy the load flow equations. The set of control variables can be represented by vector $\boldsymbol{u}$ as follows:

$$\boldsymbol{u} = \begin{bmatrix} P_{G_2} \dots P_{G_{NG}}, P_{WS_1} \dots P_{WS_{NW}}, V_{G_1} \dots V_{G_{NG}}, \\ Q_{C_1} \dots Q_{C_{NG}}, T_1 \dots T_{NT}, SVC_1 \dots SVC_{NSVC} \end{bmatrix}, \quad (7)$$

where P_G is the thermal generator active power; P_{WS} is the wind active power; V_G is the generator voltage; Q_C is the reactive power injected by the shunts compensator; T is the tap setting of transformers; SVC is the static VAR compensator; NG is the number of generators; NW is the number of wind farms; NC is the number of shunts compensators units; NT is the number of regulating transformers; $NSVC$ is the number of SVC devices.

State variables. The set of variables which describe the electrical power state can be represented by vector $\boldsymbol{x}$ as follows:

$$\boldsymbol{x} = \left[P_{Gslack}, Q_{G_1} \dots Q_{G_{NG}}, Q_{WS_1} \dots Q_{WS_{NW}}, V_{L_1} \dots V_{L_{NL}}, S_{l_1} \dots S_{l_{nl}}\right], \quad (8)$$

where P_{Gslack} is the active power generation at the slack bus; Q_G is the reactive power outputs of the generators; Q_{WS} is the reactive power outputs of the wind farms; V_L is the voltage magnitude at load bus; S_l is the apparent power flow; N_G is the total number of generators buses;

N_L is the total number of load buses or PQ buses; N_l is the total number of transmission lines.

Equality constraints. The equality constraints represent in the power system the load flow equations of the balanced powers and reflect the physics of the power system. The equality constraints can be represented as follows:

$$P_{G_i} + P_{WS_i} - P_{d_i} = V_i \sum_{j=1}^{N} V_j \left(g_{ij} \cos\delta_{ij} + z_{ij} \sin\delta_{ij} \right), \quad (9)$$

$$Q_{G_i} + Q_{WS_i} - Q_{d_i} = V_i \sum_{j=1}^{N} V_j \left(g_{ij} \sin\delta_{ij} + z_{ij} \cos\delta_{ij} \right). \quad (10)$$

Inequality constraints. The inequality constraints reflect the limiting of the power system operation. These inequality constraints can be represented as follows:

$$\begin{cases} P_{G_i}^{\min} \le P_{G_i} \le P_{G_i}^{\max}; \\ P_{WS_i}^{\min} \le P_{WS_i} \le P_{WS_i}^{\max}; \\ Q_{G_i}^{\min} \le Q_{G_i} \le Q_{G_i}^{\max}; \\ Q_{WS_i}^{\min} \le Q_{WS_i} \le Q_{WS_i}^{\max}; \\ V_{G_i}^{\min} \le V_{G_i} \le V_{G_i}^{\max}; \\ T_{NT_i}^{\min} \le T_{NT_i} \le T_{NT_i}^{\max}; \\ Q_{SVC_i}^{\min} \le Q_{SVC_i} \le Q_{SVC_i}^{\max}; \\ \left| S_{L_i} \right| \le S_{L_i}^{\max}. \end{cases} \quad (11)$$

Objective function. In this study, the objective function is to minimize the total generation cost (TGC) subject to operating constraints. The objective function is formulated as:

$$F_{tot} = \sum_{i=1}^{N} F_i(P_i) + \sum_{i=1}^{NW} C_{wr}(P_{wr}) + \sum_{i=1}^{NW} C_{p.wr}(P_{wr.av} - P_{wr}) + \sum_{i=1}^{NW} C_{r.wr}(P_{wr} - P_{wr.aw}). \quad (12)$$

In the expression of the objective function formulated in the (12), the first term denotes thermal power generation cost, second, third and last term of the objective function shows the costs of wind power, respectively. Details of all terms are explained below.

Fuel cost of the conventional generator. The cost function of the thermal generators as follows:

$$F_i(P_i) = \left(\sum_{i=1}^{N} a_i + b_i P_{G_i} + c_i P_{G_i}^2 \right), \quad (13)$$

where P_{Gi} is the active power generated from the available thermal generators; a_i, b_i and c_i are the cost coefficients of i-th generator.

The direct cost function for wind power. The grid operators pay the cost of purchasing wind power from a wind power producer based on the power purchase agreement. This cost is termed as the direct cost and is defined as follows [5]:

$$C_{wr}(P_{wr}) = d_r \cdot P_{wr}, \quad (14)$$

where d_r is the direct cost coefficient for the j-th wind generator and P_{wr} is the scheduled power output.

Cost function due to the underestimation. The underestimation situation is due when the actual wind power is higher than the estimated value. So, the utility operator needs to pay a penalty cost for not using the surplus amount of available wind power [4, 5]. The penalty cost functions due to the underestimation of available wind power represented by (15), it can be given as [26]:

$$C_{p.wr}(P_{wr.av} - P_{wr}) = k_p (P_{w.av} - P_{wr}) = = k_p \int_{P_{wr}}^{P_{r.0}} (W - P_{wr}) \cdot f_w(P_w), \quad (15)$$

where $C_{p.wr}$ is the cost associated with wind power shortage (underestimation); $P_{p.wr}$ is the actual available power output; k_p is the penalty cost coefficient due to underestimation and $f_w(P_w)$ represents the probability density function (PDF).

Cost function due to the overestimation. On contrary to the underestimation situation, the overestimation situation is due when the actual wind power is less than the estimated value. So, a spinning reserve is needed for grid operators [5]. The penalty cost function due to the overestimation of available wind power represented by (16) as follows [27]:

$$C_{r.wr}(P_{wr} - P_{wr.av}) = k_r (P_{wr} - P_{w.av}) = = k_r \int_{0}^{P_{wr}} (P_{wr} - W) \cdot f_w(P_w), \quad (16)$$

where $C_{r.wr}$ the cost associated with wind power surplus (overestimation) and k_r is the reserve cost coefficient due to overestimation.

Wind power model. The distribution function was used in this work to model and characterize the distributions of wind speed known as Weibull probability density function (PDF) [28], and can be represented as:

$$f_V(V) = \frac{k}{c} \left(\frac{v}{c} \right)^{k-1} e^{\left(-\frac{v}{c} \right)^k}, \quad (17)$$

here v is the wind speed; k and c respectively the shape factor and scale factor (m/s).

The probability density function for the continuous portion of wind energy conversion systems (WECS) power output random variable becomes as follows:

$$f_w(P_w) = \frac{k \cdot l \cdot v_{cut-in}}{c} \left(\frac{(1 + \rho \cdot 1) v_{cut-in}}{c} \right)^{k-1} \times \exp\left(- \left(\frac{(1 + \rho \cdot 1) v_{cut-in}}{c} \right)^k \right), \quad (18)$$

where $l = (v_{rated} - v_{cut-in}) / v_{cut-in}$ is the ration of linear range wind speed to cut-in wind speed; v_{cut-in} is the wind speed at which wind turbine starts to generate power; $v_{cut-off}$ is the wind speed at which the wind turbine is disconnected; v_{rated} is the wind speed at which the mechanical power output will be the rated power; $\rho = P_w / P_{wr}$ is the ratio of wind power output to rated wind power.

The probability for the discrete portion of the WECS power output is expressed by (19) and (20), respectively as follows [5, 29]:

$$f_w(P_w)=\{P_w=0\}=1-\exp\left(-\left(\frac{v_{cut-in}}{c}\right)^k\right)+ \\ +\exp\left(-\left(\frac{v_{cut-off}}{c}\right)^k\right); \quad (19)$$

$$f_w(P_w)=\{P_w=P_{wr}\}=\exp\left(-\left(\frac{v_{rated}}{c}\right)^k\right)- \\ -\exp\left(-\left(\frac{v_{cut-off}}{c}\right)^k\right); \quad (20)$$

Slime mould algorithm. A slime mould algorithm (SMA) is a new stochastic optimizer technique nature-inspired proposed in 2020 in [30]. This technique based on the oscillation mode of slime mould in nature and simulates the swarming behavior and morphology of slime mould in foraging. The SMA algorithm features a special mathematical model that uses the adaptive weight to simulates the combination of positive and negative feedback from the bio-oscillator-based propagation wave that was inspired by slime mould to form the optimal pathway to connect food. Some of the most interesting characters in the slime mould are the unique pattern based on the various food sources to create a venous network connecting them at the same time. This scheme gives the high capability of escaping from local optima solutions. The algorithm is aroused by slime mold diffusion and foraging behavior. In SMA, slime mould can approach food, depending on the smell in the air. The slime mold morphology varies, with three different forms of contraction. The following section will explain in detail the mathematical model for simulating the behavior of slime mould during the foraging [30].

Approach food. The following formulas for imitating the contraction mode is proposed to model the behavior of slime mould to approaching food according to the odor in the air as follow:

$$\overrightarrow{X(t+1)}=\begin{cases}\overrightarrow{X_B(t)}+\overrightarrow{vb}\left(\overrightarrow{W}\cdot\overrightarrow{X_A(t)}-\overrightarrow{X_B(t)}\right), r<p;\\ \overrightarrow{vc}\cdot\overrightarrow{X(t)}, r\ge p,\end{cases} \quad (21)$$

where X denotes the slime mould location; X_b is the individual emplacement with the highest odor concentration currently found; X_A and X_B are indicated two randomly selected individuals from the swarm; vb is a parameter distributed in the range of [$-a$, a]; vc decreases linearly from 1 to 0; t shows the current iteration; W represents the slime mould weight and given below by (24); p is the parameter given as follows:

$$p=\tanh\left|S(i)-DF\right|, \quad (22)$$

where $S(i)$ shows the fitness of $\overrightarrow{X}$; $i \in 1, 2, ..., n$; DF is the optimum fitness obtained in all iterations.

The parameter of a is given as follows:

$$a=\operatorname{arctanh}\left(-\left(\frac{t}{\max\_t}\right)+1\right). \quad (23)$$

The expression of $\overrightarrow{W}$ define the location of slime mould and is given as follows:

$$\overrightarrow{W(SmellIndex(i))}=\begin{cases}1+r\cdot\log\left(\frac{bF-S(i)}{bF-wF}+1\right), condition;\\ 1-r\cdot\log\left(\frac{bF-S(i)}{bF-wF}+1\right), others,\end{cases} \quad (24)$$

where *condition* denotes that $S(i)$ is ranked first half of the population; r represents the random value distributed in the range of [0, 1]; bF and wF are represented the optimal and worst fitness value obtained in the current iterative process, respectively; *SmellIndex* represents the sequence of fitness values sorted as:

$$SmellIndex=Sort(S). \quad (25)$$

Wrap food. This portion mathematically simulates the contraction mode in the slime mould venous tissue structure while searching. In this context, the higher the food concentration reached by the vein, the stronger the bio-oscillator-generated wave, the quicker the cytoplasm flows and the thicker the vein. The following mathematical formula represents updating the emplacement of slime mould:

$$\overrightarrow{X^*}=\begin{cases}rand\cdot(ub-lb)+lb, rand<z;\\ \overrightarrow{X_B(t)}+\overrightarrow{vb}\cdot\left(W\cdot\overrightarrow{X_A(t)}-\overrightarrow{X_B(t)}\right), r<p;\\ \overrightarrow{vc}\cdot\overrightarrow{X(t)}, r\ge p,\end{cases} \quad (26)$$

where lb and ub denote the lower and upper limits of the search range, respectively; *rand* denotes the random value distributed in the range of in [0, 1].

Grabble food. Slime mould is primarily dependent on the propagation wave to change the cytoplasmic flow in the veins, so they appear to be in a better concentration of food. Slime mould can approach food faster when the concentration and quality of food are high, while if the food concentration is lower, approach it more slowly, thus increasing the efficiency of slime mould in selecting the optimal source of food.

In the SMA process, the value of the parameter $\overrightarrow{vb}$ oscillates randomly in the interval between [$-a$, a] and progressively approaches zero as the iterations increase. The value of $\overrightarrow{vc}$ oscillates randomly in the interval between [–1, 1] and finally tends to be zero.

The pseudo-code of the SMA to solve the OPF problem is shown in Algorithm 1.

Algorithm 1 Pseudo-code SMA algorithm

Read the system data (bus data, line data, and generator data);
Initialize the parameters of search agents, size of the population, the maximum number of iterations, the number and position of the control variables;
Initialize the position of the slime mould X_i using (21);
While *iteration* ≤ *Max _iteration*,
Calculate the fitness of all slime mould using (26);
Update the best fitness, X_B
Calculate the W by using (24);
For each search space
Update the parameters of SMA which are: p, vb and vc;
Update the best positions of the slime mould;
Calculate the best value of the objective function (12);
End For *iter* = *iter* + 1;
End while
Return *best Fitness* found so far, X_B.

Simulations and results. To demonstrate the performance and efficiency of the SMA algorithm to solve the OPF problem by incorporating stochastic wind power and FACTS devices such as SVC, the present work aims to apply the SMA on IEEE 30-bus and Algerian 114-bus systems with different test cases study. In this context, the minimization of total fuel cost and wind power cost is considered as objective functions. The description of all these test cases can be found in the following section. All the simulations are carried out by using MATLAB 2009b and computed with specification Intel® Core™ i5 CPU@1.80 GHz with 8 GB of RAM. For establishing the robustness of the SMA algorithm, 30 independent trial runs are performed for all the test cases. In this work, the population size is 40 and the number of iterations maximal is 500.

IEEE 30-bus test system. The first test is dedicated to the standard IEEE 30-bus power system in order to verify the performance and efficiency of the SMA for the small scale power system. This system includes 6 generators unit, 41 transmission lines, 4 transformers located at lines 6-9, 4-12, 9-12, and 27-28. Nine reactive compensators are located at buses 10, 12, 15, 17, 20, 21, 23, 24, and 29. The total load is (2.834 +j·0.735) p.u.

The upper limit and lower limit variables are shown in Table 1. In this section, two different parts are considered, the first part is solving the OPF problem under normal conditions and the second part is solving the OPF problem under the contingency state.

OPF solution under normal condition. In this part**,** the SMA is applied to solve the OPF problem under the normal condition with active power loading is 283.4 MW. Three different cases are examined via SMA as follows.

Case 1: Minimization of total fuel cost. The objective function used in the first case under normal condition is to minimize the total fuel cost according to the optimal power distribution of the production units and is described by (13). Table 3 tabulates the results obtained by the SMA algorithm for Case 1. It can be seen that the optimal settings of control variables are all within their acceptable limits. Furthermore, we can also see that the fuel cost obtained by SMA is 798.9709 $/h, this value is lower and better compared to those obtained by MSA, GSO, MFO, BHBO, ALO, MSCA which are mentioned in Table 1.

Table 1

Comparison of solutions achieved using SMA and different methods for Case 1

Method	Fuel cost ($/h)
Slime mould algorithm	798.9709
Moth swarm algorithm [10]	800.5099
Glowworm Swarm Optimization [12]	799.06
Moth-Flame Optimizer [14]	799.072
Black-hole-based optimization [20]	799.921
Ant lion optimizer [31]	799.0133
Modified Sine-Cosine algorithm [32]	799.31

The convergence characteristics of the proposed method and the ALO algorithm are shown in Fig. 1. It can be seen that the SMA algorithm outperforms the ALO algorithm in terms of convergence rate towards the global optimum solution. So, the results achieved showed the SMA superior and robust compared to the ALO algorithm in order to get the best solution to solve the OPF problem.

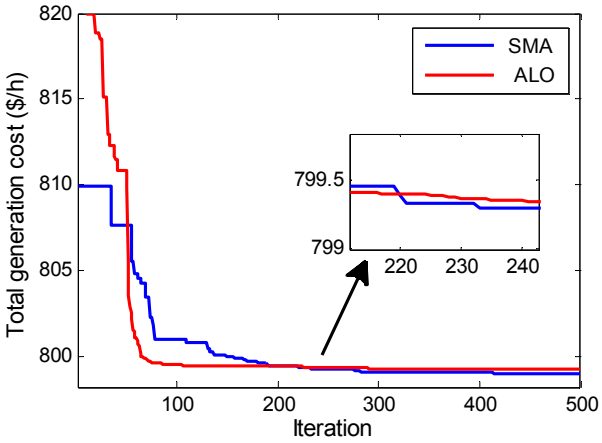

Fig. 1. Convergence characteristics of the SMA & ALO: Case 1

Case 2: Minimization of total fuel cost and wind power cost. In this test case, SMA is applied to solve the OPF problem by incorporating stochastic wind power. Thus, the objective function is minimizing the total generation cost that includes fuel cost and wind power cost. The cumulative cost, described by (13). In this case, the standard IEEE 30-bus system is considered by including two wind farms located at bus numbers 10 and 24. Moreover, the two wind farms (WFs) consist of 30 units of wind turbine generation (WTG) with a nominal power rating of each WTG is 2 MW. Thus, each WF having a total capacity of 30 MW.

Table 2 details the specification of wind turbine characteristics used in all optimization cases in this study concern with incorporating wind power for the IEEE 30-bus system [33].

Table 2

The characteristics of this wind turbine

Parameters	Value
k	2
c	3
d_r	1.3
P_{wr}	2000 kW
$v_{cut\text{-}in}$	4 m/s
v_{rated}	12 m/s
v_{cut_off}	25 m/s
$K_{p,i}$ (penalty factor)	1 $/MWh
$K_{r,i}$ (rserve factor)	4 $/MWh

Table 3 presents for case 2 the results obtained by SMA to minimize the total generation costs, which are the total fuel and wind costs. The sizing of the two wind farms can be referred to in the same table. For this case, SMA exhibit bus 10 and 24 as the optimal locations of the wind farm. At active power loading of 283.4 MW, It can be seen that the TGC produced by SMA is reduced from 798.9709 $/h to 725.7113 $/h. Moreover, the active power losses have also increased from 8.5752 MW to 6.2413 MW which is lowered by 27.21 %. Thus, SMA provides the best values to minimize the TGC and reduce the active power losses in the IEEE 30-bus test system by incorporating wind power compared to the case without the implementation of wind farms. In general, the implementation of wind farm installation to the system has significantly reduced the values of the total generation cost and the active power losses.

Table 3

Best control variable settings obtained via SMA for IEEE 30-bus system including WPG and SVC devices

Control Variables	Limits		Active power loading 283.4 MW			Active power loading 410.93 MW		
	Min	Max	Case 1	Case 2	Case 3	Case 4	Case 5	Case 6
P_{G1}(MW)	50	200	177.5784	139.3865	139.6782	199.9977	195.2207	195.2576
P_{G2}(MW)	20	80	48.6770	39.6216	39.4803	78.8218	57.6992	57.8394
P_{G5}(MW)	15	50	21.2668	18.6332	18.5144	42.4211	32.9495	32.7988
P_{G2}(MW)	10	35	21.2316	10.0000	10.0292	34.9915	34.9999	34.9896
P_{G11}(MW)	10	30	12.0890	10.0000	10.0025	29.9997	21.9266	23.1781
P_{G13}(MW)	12	40	12.0000	12.0000	12.0042	38.2946	20.3897	19.1394
P_{WS1}(MW)	0	40	–	30.0000	30.0000	–	30.0000	30.0000
P_{WS2}(MW)	0	40	–	30.0000	30.0000	–	30.0000	30.0000
V_{G1}(p.u)	0.95	1.1	1.1000	1.1000	1.1000	1.1000	1.1000	1.1000
V_{G2}(p.u)	0.9	1.1	1.0879	1.0894	1.0873	1.0843	1.0804	1.0818
V_{G5}(p.u)	0.9	1.1	1.0618	1.0644	1.0597	1.0286	1.0264	1.0263
V_{G8}(p.u)	0.9	1.1	1.0701	1.0760	1.0719	1.0616	1.0669	1.0694
V_{G11}(p.u)	0.9	1.1	1.1000	1.0539	1.0233	1.1000	1.1000	1.0964
V_{G13}(p.u)	0.9	1.1	1.1000	1.0183	1.0150	1.1000	1.0516	1.0371
T_{11}(p.u)	0.9	1.1	1.0259	1.0903	1.0989	1.0189	1.0896	1.1000
T_{12}(p.u)	0.9	1.1	0.9010	1.0286	1.0887	1.0211	1.0991	1.0993
T_{15}(p.u)	0.9	1.1	0.9803	1.0980	1.0786	1.0511	1.0997	1.0974
T_{36}(p.u)	0.9	1.1	0.9568	1.0594	1.0429	0.9609	1.0272	1.0455
Q_{C10}(Mvar)	0	5	4.3806	0.0139	1.7150	4.8813	4.1783	3.8886
Q_{C12}(Mvar)	0	5	4.7790	2.8581	0	1.9164	4.8901	0.8560
Q_{C15}(Mvar)	0	5	4.8272	0	4.7098	3.1109	3.1556	1.6088
Q_{C17}(Mvar)	0	5	4.9942	2.2721	1.4631	4.9727	4.9617	5.0000
Q_{C20}(Mvar)	0	5	2.5651	2.7844	1.0131	1.3915	1.1554	4.1684
Q_{C21}(Mvar)	0	5	2.8396	5.0000	4.8532	4.9937	0.0066	4.9944
Q_{C23}(Mvar)	0	5	3.4609	4.8785	0.5928	2.9808	2.7736	4.7325
Q_{C24}(Mvar)	0	5	4.9957	0.2167	1.8172	4.6307	1.3769	0.0423
Q_{C29}(Mvar)	0	5	1.1562	0.9389	0.4900	1.1981	1.2900	4.8493
Q_{WS1}(Mvar)	–15	40	–	–3.9319	39.4803	–	4.7442	57.8394
Q_{WS2}(Mvar)	–15	40	–	3.3754	0.8719	–	10.3240	32.7988
Q_{SVC30}(Mvar)	–25	25	–	–	5.6479	–	–	6.6716
Total generation cost ($/h)			798.9709	725.7113	725.8855	1339.4776	1198.1826	1198.2092
Power losses (MW)			8.5752	6.2413	6.3087	13.5964	12.2555	12.2729
Voltage deviation (p.u.)			1.4494	0.6285	0.5195	0.7413	0.6066	0.5465
Reserved real power			–	53.5074	53.5074	–	53.5074	53.5074

The convergence curves of the SMA and ALO for case 2 are shown in Fig. 2, which allows us to note, in the first place, that the SMA converges towards the global optimum value at iteration 120 compared to the ALO, that the convergence towards the optimal solution is reached at iteration 270.

Case 3: Minimization of fuel cost and wind power cost by considering the SVC device. In this case study, SMA is applied for solving the OPF problem by incorporating wind power and SVC devices. The optimal location of the SVC device for the IEEE 30-bus system found by SMA is bus N°30. The objective function used is to minimize the TGC as described by (13). From this case, It can be seen that the voltage deviation is reduced from 1.4494 p.u (case 1) and 0.6285 (case 2) to 0.5428 p.u. The voltage profile obtained by the SMA algorithm for cases 2 and 3 is shown in Fig. 3. It is seen that the effect of the SVC device to improve the profile voltage, especially in the busses far from generators units such as bus N°25 until bus N°30.

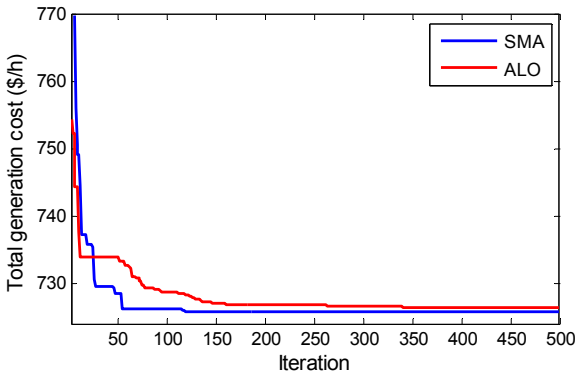

Fig. 2. Convergence characteristics of the SMA & ALO: Case 2

OPF solution under the contingency state. In this part, the SMA is applied to solve the OPF problem under

the contingency state, which is increased loading at 45 %. Thus, the active power loading is 410.93 MW. Three different cases are considered for this part.

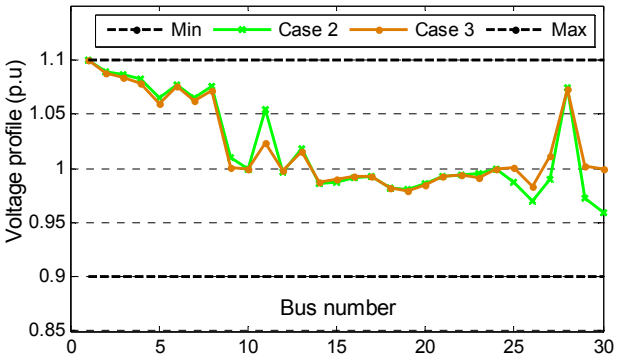

Fig. 3. Profile Voltage magnitudes for case 2 and case 3

Case 4: Minimization of total fuel cost. In this case, the objective function is to optimize the total fuel cost in the IEEE 30-bus system with increased loading at 45 % and is described by (16) addition to the penalty of line power. From the results given by the SMA algorithm for the case N°5, It can be seen that most generators work near their maximum limits, due to the increased load compared to the results given in case 1 without increased load. Moreover, we can also see that the fuel cost, active power losses, and voltage deviation are increased as presented in Table 3. The convergence characteristics of the SMA and ALO for case 4 are shown in Fig. 4.

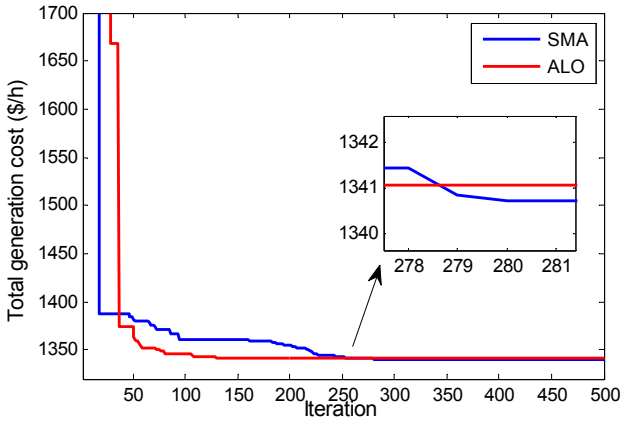

Fig. 4. Convergence characteristics of the SMA & ALO: Case 4

Case 5: Minimization of total fuel cost and wind power cost. The minimization of total fuel cost and wind power cost, in this case, is formulated as the objective function, which is described by (13). At higher active power loading of 410.90 MW, SMA provides 1198.1826 $/h for the TGC, this value better than a value obtained in a case without incorporating wind power. On the other hand, the implementation of wind farms has reduced the active power losses and the deviation voltage in the system.

The convergence characteristics of the SMA and ALO for case 5 are shown in Fig. 5. From this figure, it demonstrates that the SMA algorithm can converge to the global optimum at iteration 170, while ALO towards the optimal solution is reached at iteration 230.

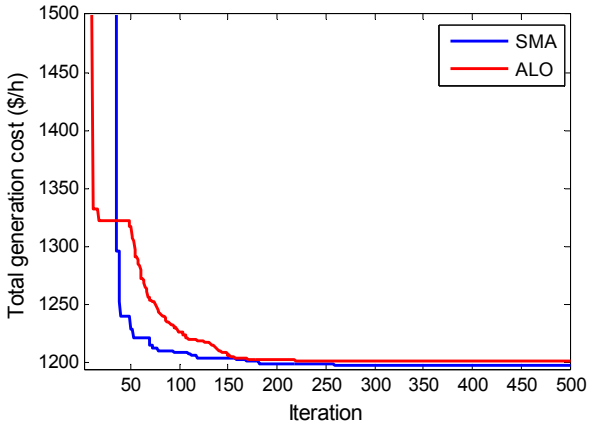

Fig. 5. Convergence characteristics of the SMA & ALO: Case 5

Case 6: Minimization of total fuel cost and wind power cost by considering the SVC device. In this case, we have study the influence of SVC devices on a power system to improve the voltage profile. The voltage profile for case 5 and case 6 are shown in Fig. 6. Unlike case 5 where profile voltage decreases after overloading, adding the SVC to the power system, in this case, improves the voltage as seen in Fig 6. Through the given results, we note that the effect of SVC is significant in the case of increased load.

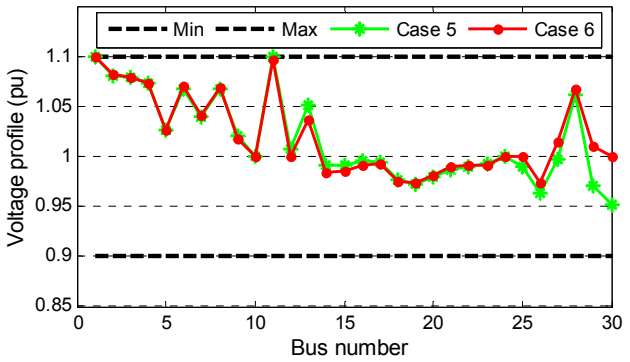

Fig. 6. Profile voltage magnitudes for case 5 and case 6

Algerian electrical network system. In order to verify the performance and efficiency of the ALO to solve nonlinear problems in larger-scale dimensions, OPF is performed on the Algerian electrical network system. This system includes 15 generators, 175 transmission lines, and 16 located from line 160 to line 175. The technical and economic parameters of generator units of the Algerian electrical network system are presented in [34].

Case 7: Minimization of total fuel cost. In this case, SMA is tested to identify the optimal fuel cost on the large-scale Algerian electrical network system with 114 buses. Table 4 presents the optimal settings of control variables reached by SMA with three different cases taking into consideration the vector of control variables contains the active powers generated and the generator voltages. The best value of fuel cost obtained by SMA for the vector of control variables contains the active powers generated is 18914.105 $/h and better than other methods as well as previously reported methods in Table 5.

The convergence characteristics of the proposed algorithm and ALO algorithm for case 7 are shown in Fig. 7. It can be seen that the SMA algorithm outperforms the ALO algorithm in terms of convergence rate towards the global optimum solution.

Table 4

Best control variable settings obtained via SMA for ALG 114-bus system including WPG and SVC devices

Control Variables	Case 7	Case 8	Case 9	Control Variables	Case 7	Case 8	Case 3
P_{G4}(MW)	451.3078	444.8246	446.5335	V_{G4}(p.u)	1.0997	1.1000	1.0999
P_{G5}(MW)	451.1405	446.1754	443.8411	V_{G5}(p.u)	1.1000	1.1000	1.1000
P_{G11}(MW)	99.9998	99.9992	99.9993	V_{G11}(p.u)	1.0954	1.0990	1.0993
P_{G15}(MW)	193.3981	190.5629	188.6959	V_{G15}(p.u)	1.1000	1.1000	1.0993
P_{G17}(MW)	446.9078	439.3309	441.6877	V_{G17}(p.u)	1.1000	1.1000	1.1000
P_{G19}(MW)	194.8571	190.8661	189.4341	V_{G19}(p.u)	1.0599	1.0523	1.0590
P_{G22}(MW)	191.8038	190.0866	186.7558	V_{G22}(p.u)	1.0620	1.0589	1.0683
P_{G52}(MW)	188.5324	186.9000	185.9111	V_{G52}(p.u)	1.0661	1.0622	1.0668
P_{G80}(MW)	190.4592	184.5212	186.0970	V_{G80}(p.u)	1.1000	1.1000	1.0998
P_{G83}(MW)	187.8661	181.9296	183.6420	V_{G83}(p.u)	1.1000	1.1000	1.1000
P_{G98}(MW)	188.6026	183.2775	184.3464	V_{G98}(p.u)	1.1000	1.1000	1.1000
P_{G100}(MW)	600.0000	599.9998	600.0000	V_{G100}(p.u)	1.1000	1.1000	1.1000
P_{G101}(MW)	200.0000	200.0000	200.0000	V_{G101}(p.u)	1.1000	1.1000	1.1000
P_{G109}(MW)	100.0000	99.9995	99.9985	V_{G109}(p.u)	1.1000	1.1000	1.0998
P_{G111}(MW)	99.9976	100.0000	100.0000	V_{G111}(p.u)	1.0701	1.0650	1.0792
P_{WS1}(MW)	–	15.0000	15.0000	Q_{SVC68}(Mvar)	–	–	22.000
P_{WS2}(MW)	–	30.0000	29.9999	Q_{SVC89}(Mvar)	–	–	32.800
		Case 1		Case 2		Case 3	
Fuel cost ($/h)		18914.105		18624.9978		18610.7234	
Power losses (MW)		57.8726		56.4733		54.9422	
Voltage deviation (p.u.)		4.9714		4.8197		4.5968	
Reserved real power		–		41.0227		41.0227	

Table 5

Comparison of solutions achieved using SMA and different methods for Case 7

Method	Fuel cost ($/h)
Slime mould algorithm	18914.105
Differential evolution [34]	19203.340
Grey wolf optimizer [35]	19171.958
Hybrid GA-DE-PS [36]	19199.444
M-objective ant lion algorithm [37]	19355.859

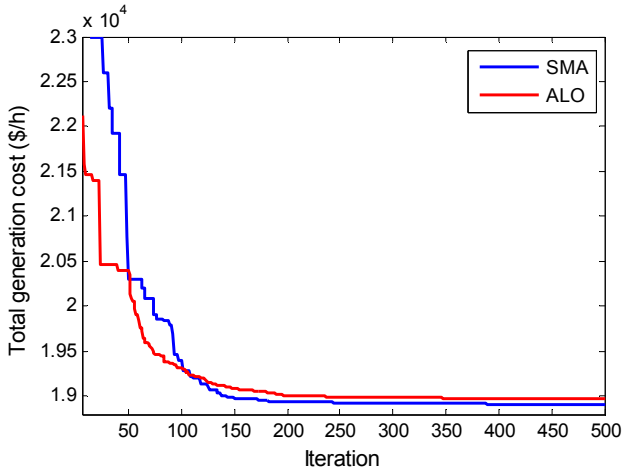

Fig. 7. Convergence characteristics of the SMA & ALO: Case 7

Case 8: Minimization of total fuel cost and wind power cost. In this case, SMA is applied to solve the OPF problem on the large-scale power system by incorporating stochastic wind power. The Algerian power system ALG 114-bus is considered by including two wind generators located at busses 99 (Setif) and 107 (Djelfa). Moreover, the two wind farms (WF) consist of 40 units of wind turbine generation (WTG) are connected to the system at busses 10 and 24 with a nominal power rating of each WTG is 1.5 MW. Weibull settings for the sites that have been chosen are taken from [38]. The choice of the turbine has been set for General Electric GE 1,5-77 machines. The characteristics of this wind turbine are shown in Table 6.

Table 6

The characteristics of this wind turbine

Parameters	Wind turbine1	Wind turbine
k	1.425	2.008
c	4.083	5.178
d_r	1.75	2
P_{wr}	15 MW	30 MW
$v_{cut\text{-}in}$	3.5 m/s	3.5 m/s
v_{rated}	12 m/s	12 m/s
$v_{cut\text{-}off}$	25 m/s	25 m/s
$K_{p,j}$ (penalty factor)	1.5 $/MWh	1.5 $/MWh
$K_{r,j}$ (rserve factor)	3 $/MWh	3 $/MWh

Table 4 summarizes the best results reached by SMA to minimize total generation cost, reduce active power losses and improve the voltage profile by incorporating two wind farms. Based on the results achieved by the SMA in case 7 compared to case 8, the incorporation of wind farms into the system in the ALG 114 system gave more significant profit in TGC and reducing active power losses. The convergence characteristics of the SMA for case 8 are shown in Fig. 8. The convergence of the SMA is reached in the first 170 iterations, while the convergence of the ALO towards the optimal solution is reached at iteration 230.

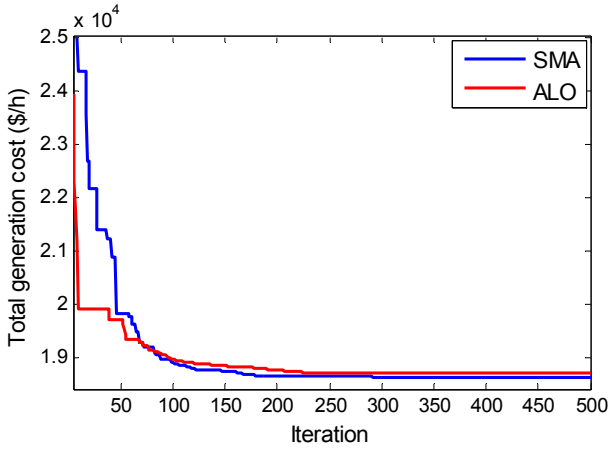

Fig. 8. Convergence characteristics of the SMA & ALO: Case 8

Case 9: Minimization of total fuel cost and wind power cost by considering the SVC device. In order to illustrate the effectiveness of the SMA in presence of SVC devices on the power system, the ALG 114-bus is considered by including two SVC devices at busses N°68 (Sedjerara) and bus N°89 (Souk Ahras). These locations of SVC devices are considered the optimal placement in the Algerian 114-bus system found by the SMA algorithm. After the results of the simulation, the installation of the SVC improved considerably the total generation cost, the active power loss. Figure 9 represents that the effect of SVC devices is significant in the Algerian 114-bus system to maintain the voltages within the acceptable limits.

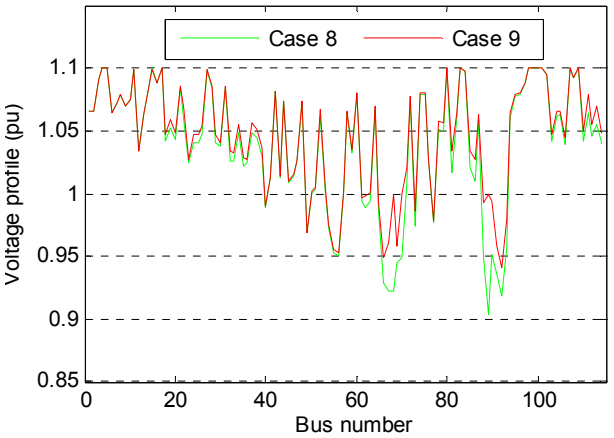

Fig. 9. Profile voltage magnitudes for case 8 and case 9

Conclusion. This paper proposed a recent metaheuristic technique called a slime mould algorithm to solve the optimal power flow problem incorporating stochastic wind power and static VAR compensator devices. In this study, nine cases have been considered and examined via the proposed algorithm on the IEEE 30-bus system and practical Algerian power system ALG 114-bus. The objective function solved is a minimization of the total generation cost that includes fuel cost and wind power cost. Also, the nature of the wind output function used is based on the Weibull probability distribution model. For the case without considering wind power and static VAR compensator devices, it is worth mentioning that the proposed algorithm is capable of achieving and getting the best global optimal solution for both of the testing systems compared to the other methods in the literature mentioned in this paper. With considering wind power and SVC devices, the numerical results obtained show a better performance of the proposed algorithm to solve the optimal power flow problem compared to the ant lion optimizer algorithm. Additionally, incorporating the wind power and static VAR compensator device has a high influence on the power system through minimize the total generation cost, reduce the active power loss as well as improve the voltage profile. Thus, the results obtained prove the merits and efficiency of the proposed algorithm to solve the stochastic optimal power flow problem.

REFERENCES

1. Bhatia S.C. Energy resources and their utilization. *Advanced Renewable Energy Systems*, pp. 1–31, 2014. **doi: 10.1016/B978-1-78242-269-3.50001-2**.

2. Talari S., Shafie-khah M., Osório G.J., Aghaei J., Catalão J.P.S. Stochastic modelling of renewable energy sources from operators' point-of-view: A survey. *Renewable and Sustainable Energy Reviews*, 2018, vol. 81, part 2, pp. 1953-1965. **doi: 10.1016/j.rser.2017.06.006.**

3. Roy R., Jadhav H.T. Optimal power flow solution of power system incorporating stochastic wind power using Gbest guided artificial bee colony algorithm. *International Journal of Electrical Power & Energy Systems*, 2015, vol. 64, pp. 562-578. **doi: 10.1016/j.ijepes.2014.07.010.**

4. Elattar E.E. Optimal Power Flow of a Power System Incorporating Stochastic Wind Power Based on Modified Moth Swarm Algorithm. *IEEE Access*, 2019, vol. 7, pp. 89581-89593. **doi: 10.1109/ACCESS.2019.2927193.**

5. Biswas P.P., Suganthan P.N., Amaratunga G.A.J. Optimal power flow solutions incorporating stochastic wind and solar power. *Energy Conversion and Management*, 2017, vol. 148, pp. 1194-1207. **doi: 10.1016/j.enconman.2017.06.071.**

6. Panda A., Tripathy M. Security constrained optimal power flow solution of wind-thermal generation system using modified bacteria foraging algorithm. *Energy*, 2015, vol. 93, pp. 816-827. **doi: 10.1016/j.energy.2015.09.083**.

7. Ahmad M., Javaid N., Niaz I.A., Shafiq S., Rehman O.U., Hussain H.M. Application of bird swarm algorithm for solution of optimal power flow problems. *12-th International Conference on Complex, Intelligent, and Software Intensive Systems (CISIS-2018). Advances in Intelligent Systems and Computing*, vol 772, pp. 280-291. Springer, Cham. **doi: 10.1007/978-3-319-93659-8_25.**

8. Duman S., Li J., Wu L., Guvenc U. Optimal power flow with stochastic wind power and FACTS devices: a modified hybrid PSOGSA with chaotic maps approach. *Neural Computing and Applications,* 2019, vol. 32, no. 12, pp. 8463-8492. **doi: 10.1007/s00521-019-04338-y.**

9. El-Fergany A.A., Hasanien H.M. Salp swarm optimizer to solve optimal power flow comprising voltage stability analysis. *Neural Computing and Applications,* 2019, vol. 32, no. 9, pp. 5267-5283. **doi: 10.1007/s00521-019-04029-8.**

10. Mohamed A.-A.A., Mohamed Y.S., El-Gaafary A.A., Hemeida A.M. Optimal power flow using moth swarm algorithm. *Electric Power Systems Research*, 2017, vol. 142, pp. 190-206. **doi: 10.1016/j.epsr.2016.09.025.**

11. Biswas P.P., Suganthan P.N., Mallipeddi R., Amaratunga G.A.J. Optimal power flow solutions using differential evolution algorithm integrated with effective constraint handling techniques. *Engineering Applications of Artificial Intelligence*, 2018, vol. 68, pp. 81-100. **doi: 10.1016/j.engappai.2017.10.019.**

12. Surender Reddy S., Srinivasa Rathnam C. Optimal Power Flow using Glowworm Swarm Optimization," *International Journal of Electrical Power & Energy Systems*, 2016, vol. 80, pp. 128-139. **doi: 10.1016/j.ijepes.2016.01.036.**

13. Abaci K., Yamacli V. Differential search algorithm for solving multi-objective optimal power flow problem. *International Journal of Electrical Power & Energy Systems*, 2016, vol. 79, pp. 1-10. **doi: 10.1016/j.ijepes.2015.12.021.**

14. Trivedi I.N., Jangir P., Parmar S.A., Jangir N. Optimal power flow with voltage stability improvement and loss reduction in power system using Moth-Flame Optimizer. *Neural Computing and Applications*, 2016, vol. 30, no. 6, pp. 1889-1904. **doi: 10.1007/s00521-016-2794-6.**

15. Pulluri H., Naresh R., Sharma V. A solution network based on stud krill herd algorithm for optimal power flow problems. *Soft Computing*, 2016, vol. 22, no. 1, pp. 159-176. **doi: 10.1007/s00500-016-2319-3.**

16. Jadon S.S., Bansal J.C., Tiwari R., Sharma H. Artificial bee colony algorithm with global and local neighborhoods. *International Journal of System Assurance Engineering and Management*, 2014, vol. 9, no. 3, pp. 589-601. **doi: 10.1007/s13198-014-0286-6.**

17. Duman S. Symbiotic organisms search algorithm for optimal power flow problem based on valve-point effect and prohibited zones. *Neural Computing and Applications*, 2016, vol. 28, no. 11, pp. 3571-3585. **doi: 10.1007/s00521-016-2265-0**.

18. Bouchekara H.R.E.H., Chaib A.E., Abido M.A., El-Sehiemy R.A. Optimal power flow using an Improved Colliding Bodies Optimization algorithm. *Applied Soft Computing*, 2016, vol. 42, pp. 119-131. **doi: 10.1016/j.asoc.2016.01.041.**

19. Hariharan T., Sundaram K.M. Optimal Power Flow Using Firefly Algorithm with Unified Power Flow Controller. *Circuits and Systems*, 2016, vol. 07, no. 08, pp. 1934-1942. **doi: 10.4236/cs.2016.78168.**

20. Bouchekara H.R.E.H. Optimal power flow using black-hole-based optimization approach. *Applied Soft Computing*, 2014, vol. 24, pp. 879-888. **doi: 10.1016/j.asoc.2014.08.056.**

21. Bouchekara H.R.E.H., Abido M.A., Chaib A.E., Mehasni R. Optimal power flow using the league championship algorithm: A case study of the Algerian power system. *Energy Conversion and Management*, 2014, vol. 87, pp. 58-70. **doi: 10.1016/j.enconman.2014.06.088.**

22. Mohan T.M., Nireekshana T. A Genetic algorithm for solving optimal power flow problem. *Procedings 2019 3rd International conference on Electronics, Communication and Aerospace Technology (ICECA)*, 2019, pp. 1438-1440. **doi: 10.1109/ICECA.2019.8822090.**

23. Bentouati B., Chettih S., Jangir P., Trivedi I.N. A solution to the optimal power flow using multi-verse optimizer. *Journal of Electrical Systems*, 2016, vol. 12, no. 4, pp. 716-733,.

24. Ren P., Li N. Optimal power flow solution using the Harmony search algorithm. *Applied Mechanics and Materials*, 2014, vol. 599-601, pp. 1938-1941. **doi: 10.4028/www.scientific.net/AMM.599-601.1938.**

25. Ghosh I., Roy P.K. Application of earthworm optimization algorithm for solution of optimal power flow. *2019 International Conference on Opto-Electronics and Applied Optics (Optronix)*, 2019, vol. 1, no. 1, pp. 1-6. **doi: 10.1109/OPTRONIX.2019.8862335.**

26. Hetzer J., Yu D.C., Bhattarai K. An Economic Dispatch Model Incorporating Wind Power. *IEEE Transactions on Energy Conversion*, 2008, vol. 23, no. 2, pp. 603-611. **doi: 10.1109/tec.2007.914171.**

27. Makhloufi S., Mekhaldi A., Teguar M. Three powerful nature-inspired algorithms to optimize power flow in Algeria's Adrar power system. *Energy*, 2016, vol. 116, pp. 1117-1130. **doi: 10.1016/j.energy.2016.10.064.**

28. Panda A., Tripathy M. Optimal power flow solution of wind integrated power system using modified bacteria foraging algorithm. *International Journal of Electrical Power & Energy Systems*, 2014, vol. 54, pp. 306-314. **doi: 10.1016/j.ijepes.2013.07.018.**

29. Teeparthi K., Vinod Kumar D.M. Multi-objective hybrid PSO-APO algorithm based security constrained optimal power flow with wind and thermal generators. *Engineering Science and Technology, an International Journal*, 2017, vol. 20, no. 2, pp. 411-426. **doi: 10.1016/j.jestch.2017.03.002.**

30. Li S., Chen H., Wang M., Heidari A.A., Mirjalili S. Slime mould algorithm: A new method for stochastic optimization. *Future Generation Computer Systems*, 2020, vol. 111, pp. 300-323. **doi: 10.1016/j.future.2020.03.055.**

31. Kouadri R., Slimani L., Bouktir T., Musirin I. Optimal Power Flow Solution for Wind Integrated Power in presence of VSC-HVDC Using Ant Lion Optimization. *Indonesian Journal of Electrical Engineering and Computer Science*, 2018, vol. 12, no. 2, p. 625. **doi: 10.11591/ijeecs.v12.i2.pp625-633.**

32. Attia A.-F., El Sehiemy R.A., Hasanien H.M. Optimal power flow solution in power systems using a novel Sine-Cosine algorithm. *International Journal of Electrical Power & Energy Systems*, 2018, vol. 99, pp. 331-343. **doi: 10.1016/j.ijepes.2018.01.024.**

33. Haddi S., Bouketir O., Bouktir T. Improved Optimal Power Flow for a Power System Incorporating Wind Power Generation by Using Grey Wolf Optimizer Algorithm. *Advances in Electrical and Electronic Engineering*, 2018, vol. 16, no. 4, pp. 471-488. **doi: 10.15598/aeee.v16i4.2883.**

34. Slimani L., Bouktir T. Optimal Power Flow Solution of the Algerian Electrical Network using Differential Evolution Algorithm. *TELKOMNIKA (Telecommunication Computing Electronics and Control)*, 2012, vol. 10, no. 2, p. 199. **doi: 10.12928/telkomnika.v10i2.778.**

35. Kouadri R., Musirin I., Slimani L., Bouktir T. OPF for large scale power system using ant lion optimization: a case study of the Algerian electrical network. *IAES International Journal of Artificial Intelligence (IJ-AI)*, 2020, vol. 9, no. 2, p. 252. **doi: 10.11591/ijai.v9.i2.pp252-260.**

36. Mahdad B., Srairi K. Solving practical economic dispatch using hybrid GA–DE–PS method. *International Journal of System Assurance Engineering and Management*, 2013, vol. 5, no. 3, pp. 391-398. **doi: 10.1007/s13198-013-0180-7.**

37. Herbadji O., Slimani L., Bouktir T. Optimal power flow with four conflicting objective functions using multiobjective ant lion algorithm: A case study of the algerian electrical network. *Iranian Journal of Electrical and Electronic Engineering*, 2019, vol. 15, no. 1, pp. 94-113. **doi: 10.22068/IJEEE.15.1.94.**

38. Derai A., Diaf A.K.S. Etude de faisabilité technico-économique de fermes éoliennes en Algérie. *Rev. des Energies Renouvelables*, 2017, vol. 20, no. 4, pp. 693-712. (Fra).

Received 11.08.2020
Accepted 02.11.2020
Published 24.12.2020

Ramzi Kouadri[1], *Ph.D Student,*
Linda Slimani[1], *Professor,*
Tarek Bouktir[1], *Professor,*
[1] Department of Electrical Engineering,
University of Ferhat Abbas Setif 1,
19000, Setif, Algeria.
e-mail: ramzikouadri@univ-setif.dz,
slimaniblinda@gmail.com,
tbouktir@univ-setif.dz